

# Water Dispersible, Positive and Negatively Charged MoS<sub>2</sub> Nanosheets: Surface Chemistry and the Role of Surfactant Binding

*Amit Gupta, Vaishali Arunachalam and Sukumaran Vasudevan\**

Department of Inorganic and Physical Chemistry

Indian Institute of Science, Bangalore 560012,

INDIA

\* Author to whom correspondence may be addressed. E-mail: [svipc@ipc.iisc.ernet.in](mailto:svipc@ipc.iisc.ernet.in). Tel:  
+91-80-2293-2661. Fax: +91-80-2360-1552/0683;

**Supporting Information**

## **Content**

S1. Experimental methods

S2. Zeta potential measurements at different surfactant concentrations

S3. Particle size distribution of MoS<sub>2</sub>-CTAB dispersions from AFM measurements

S4. Particle size distribution of MoS<sub>2</sub>-CTAB dispersions from TEM

S5. Exit wave phase reconstruction of TEM images of MoS<sub>2</sub> nanosheets

S6. NOESY spectra of surfactant (CTAB and SDS) solutions

## S1 Experimental methods

Exfoliation of MoS<sub>2</sub> (Sigma Aldrich, <2 μm) was achieved by dispersing 330mg of the solid in 30ml 1% surfactant solution, of either CTAB or SDS, in water followed by sonication for 8 hours in a 100 W bath sonicator. After sonication a deep green dispersion was obtained that was stable for weeks without any flocculation. For the microscopy and NMR characterization measurements the dispersions were subjected to differential centrifugation to narrow down the size distribution. Centrifugation was carried out in two steps, at 4000 and 7000 RPM, with the precipitates obtained after 7000 RPM being used for all the studies.

### Physical characterization

The zeta potential of the as-prepared dispersions were measured on a NanoBrook ZetaPALS instrument in the electrophoretic light scattering (ELS) mode using a 660 nm red diode laser. For this wavelength the refractive index of MoS<sub>2</sub> was taken to be 6.1 . For recording atomic force microscope (AFM) images the centrifuged dispersion was drop coated on a freshly cleaved mica, dried and then soaked in ethanol, to remove excess surfactant, and subsequently dried under vacuum. For the TEM analysis the MoS<sub>2</sub> –surfactant dispersion was drop coated on a formvar 3mm copper grid. After drying the grid was washed with ethanol to remove any excess surfactant and dried under vacuum. AFM images were recorded on Veeco MultiMode IV microscope in tapping mode while TEM images were recorded on a JEOL JEM 2100F electron microscope equipped with a Olympus KeenView K2 CCD camera, at an acceleration voltage of 200 kV.

The <sup>1</sup>H NMR spectra of MoS<sub>2</sub> -CTAB and MoS<sub>2</sub> – SDS were recorded after re-dispersion in D<sub>2</sub>O. Spectra were recorded on a Bruker Avance 400 NMR spectrometers. All 1D and 2D

spectra were recorded using standard pulse sequences from the Bruker pulse program library in TopSpin 1.3. The spectra were referenced to TMS. The DOSY spectra were acquired after application of a 2 ms gradient pulse followed by a diffusion delay of 400 ms of diffusion time. The DOSY measurements were processed using the Topspin3.2 DOSY processing software. The 2D NOESY were recorded on JEOL ECX500II spectrometer with an optimized mixing time of 400ms for the MoS<sub>2</sub>-CTAB dispersion and 300ms for MoS<sub>2</sub>-SDS dispersion. The 2D NOESY were recorded using a phase sensitive Pulse Field Gradient (PFG) zzfilter and dante pre-saturation pulse sequence for water suppression and to remove artifacts arising from zero quantum coherences between spins that are J-coupled.

## S2 Zeta potential measurements at different surfactant concentrations

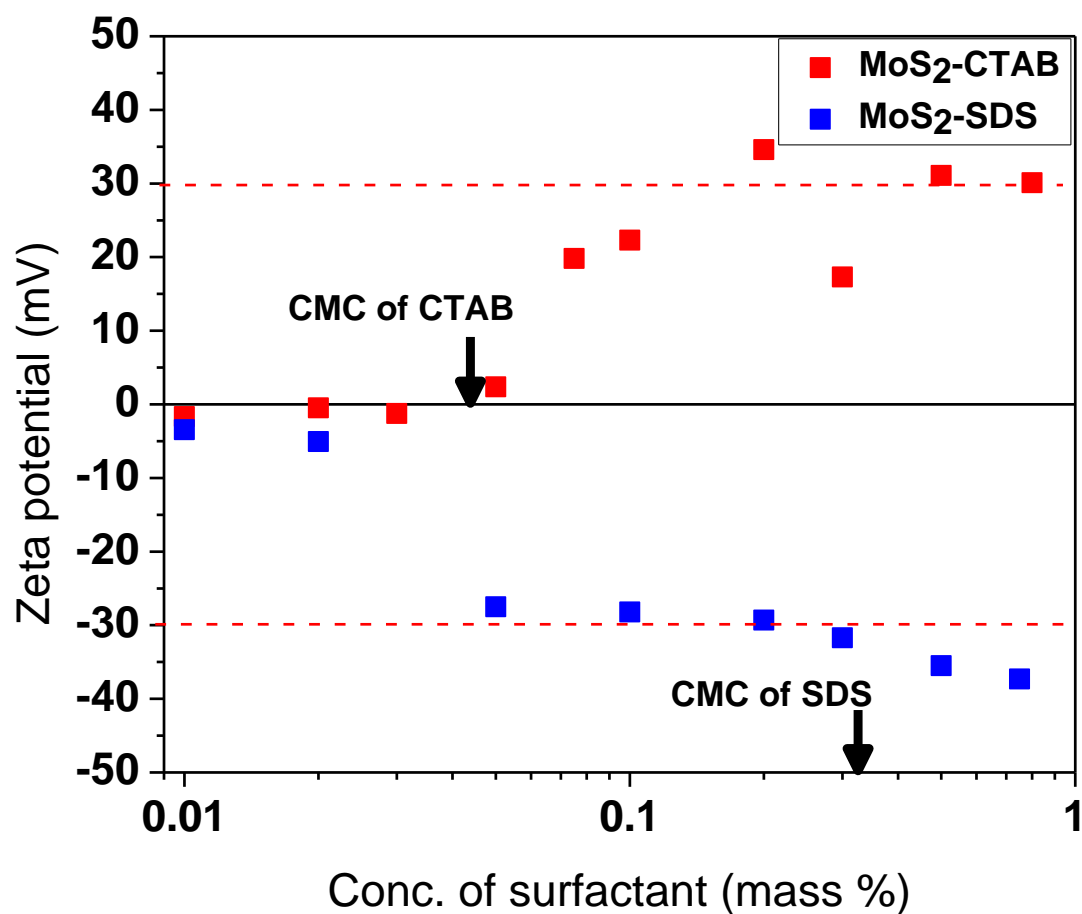


**Figure S1.** Zeta potential measurements of MoS<sub>2</sub>- CTAB and MoS<sub>2</sub>-SDS dispersions at different surfactant concentrations. The arrows indicate the CMC values for CTAB and SDS. Stable dispersions are formed when the zeta potential is greater than 30mV or less than -30mV (indicated by the dashed lines in the figure).

### S3 Particle size distribution of MoS<sub>2</sub>-CTAB dispersions from AFM measurements

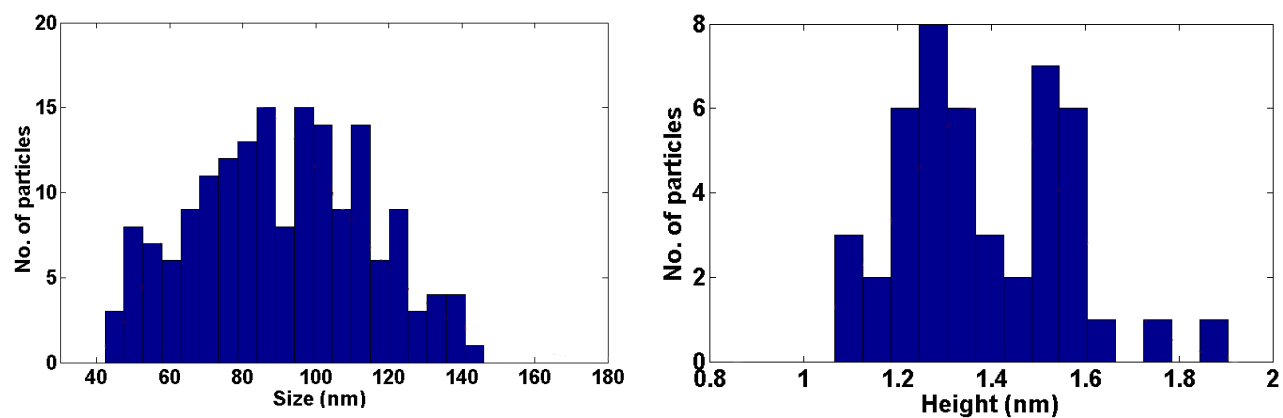


**Figure S2.** Lateral and vertical size distribution histograms as obtained from AFM images of MoS<sub>2</sub>-CTAB dispersions

### S4 Particle size distribution of MoS<sub>2</sub>-CTAB dispersions from TEM images

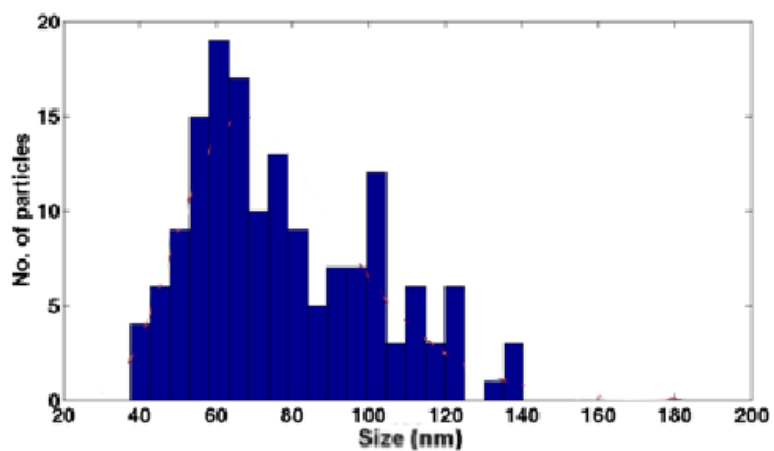


**Figure S3.** Particle size histogram obtained from TEM images of MoS<sub>2</sub>-CTAB dispersions

## **S5 Exit wave phase reconstruction of TEM images**

The exit wave procedure using the a series of defocus images was used for the TEM image reconstruction.<sup>S1</sup> Eleven images were acquired at different defocus values, as indicated in Figure S3. The 2-fold astigmatism and coma aberration of the images were aligned; higher order aberration (3-fold aberration and coma). were assumed to be zero Spherical aberration coefficient  $C_s$  was estimated to be 0.95mm by the beam tilt method whereas the chromatic aberration energy spread was taken to be 3eV (from JEOL user manual).<sup>S2</sup> Beam convergence angle was conservatively estimated to be below 1 mrad, hence a value of 1 mrad was used in the calculations. Modulus transfer function of the CCD camera was obtained from a shadow image of the beam blocker<sup>S3</sup>. Individual defocus of each image in Figure S3 was precisely determined by fitting estimated parameters to Thon rings.<sup>S4</sup> Image registration to sub-pixel accuracy was achieved through phase correlation method. Exit wave reconstruction was achieved from Inverse Wiener Filter method.<sup>S5</sup> Figure S4 shows the reconstructed image with intensity profile along the marked line being displayed in inset.

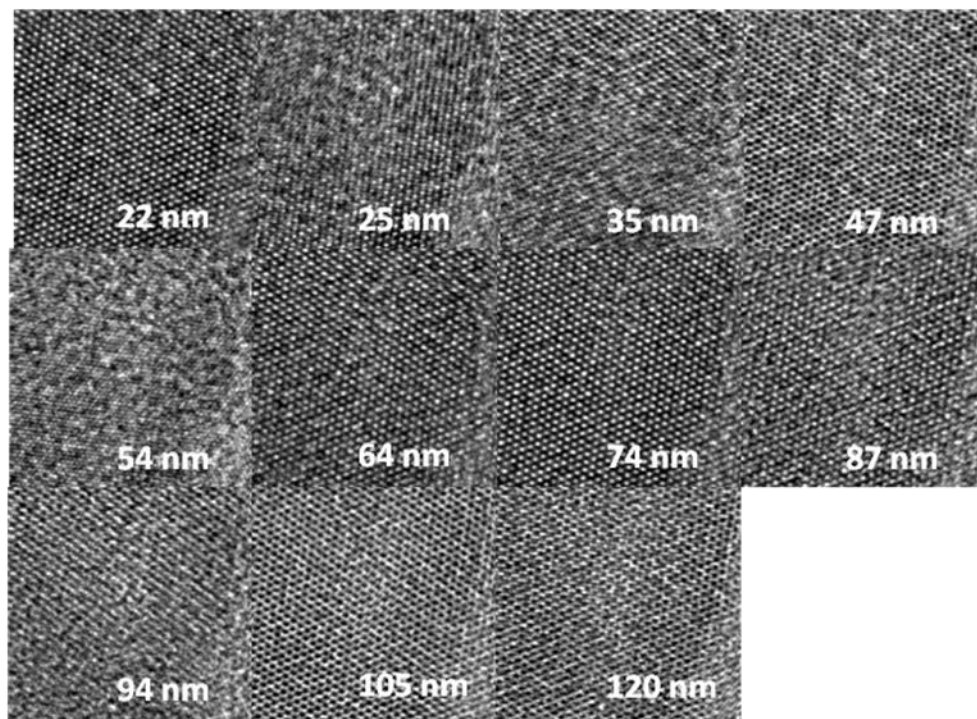


**Figure S4.** Images of MoS<sub>2</sub>-CTAB acquired at different defocus values as indicated.

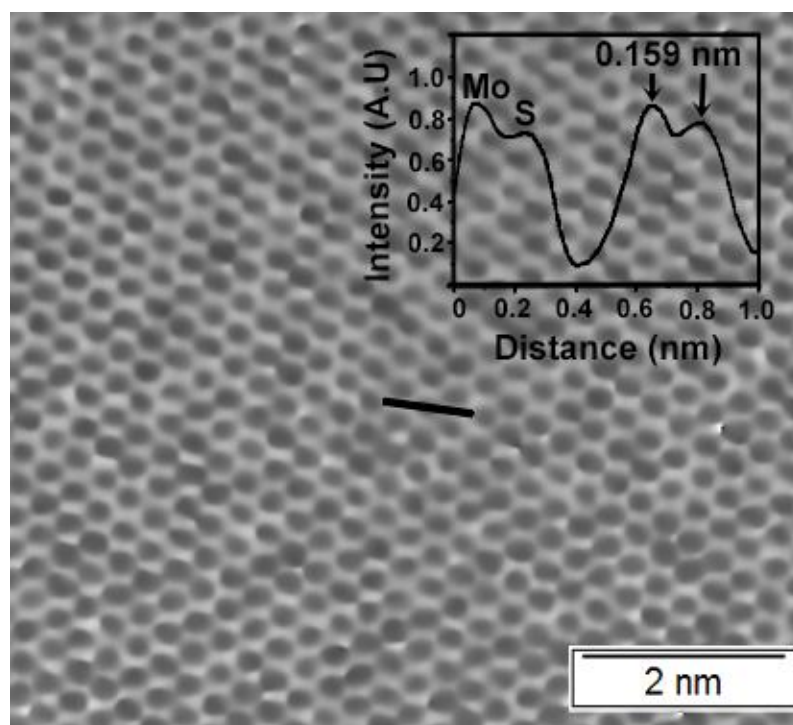


**Figure S5.** Reconstructed Exit wave/Phase from the images shown in Figure S3. The inset shows the intensity profile of the reconstructed wave along the marked line. The Mo and S atoms may be clearly distinguished.



S6 NOESY spectra of surfactant (CTAB and SDS) solutions

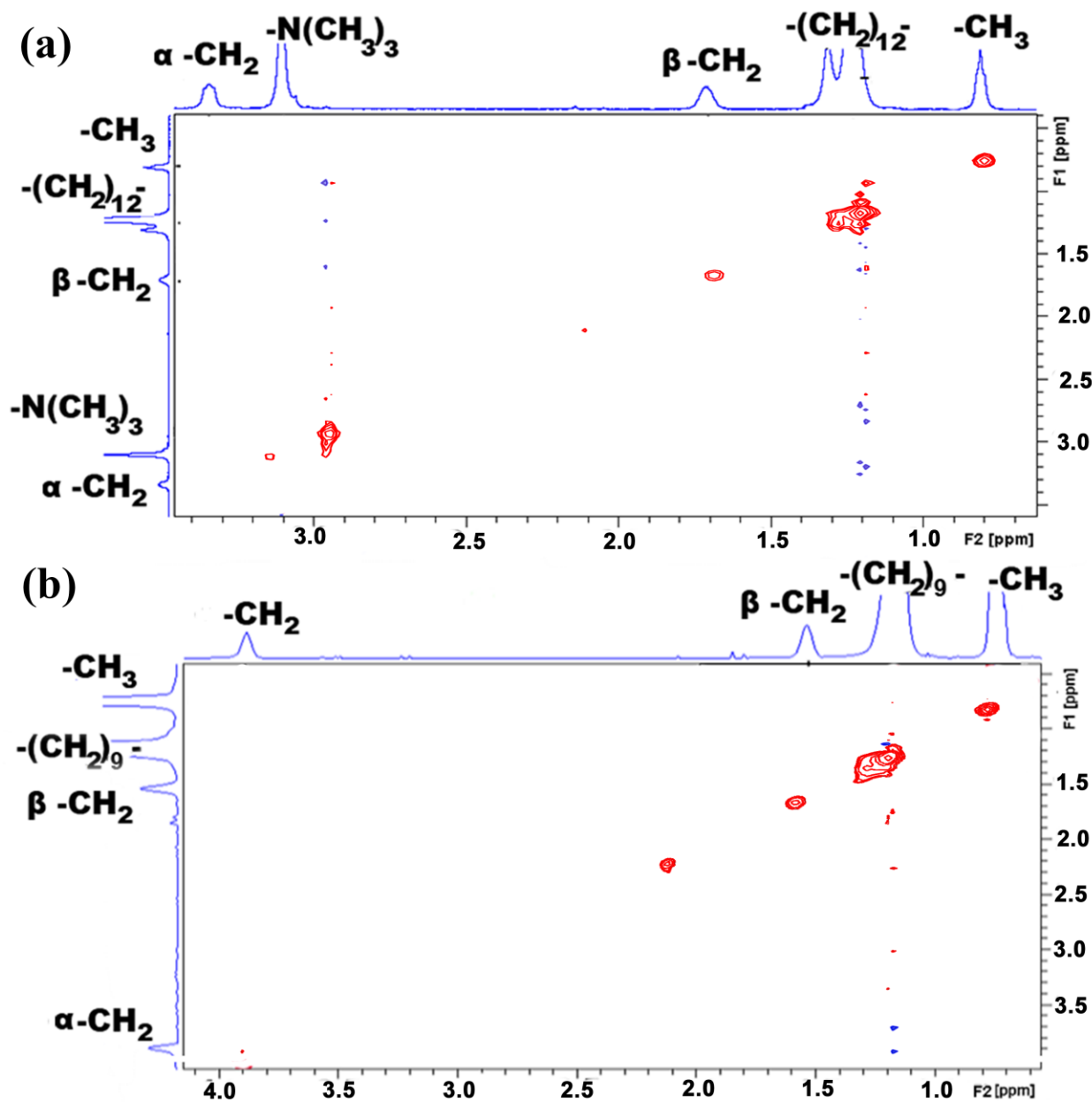


Figure S6. NOESY spectra of (a) CTAB and (b) SDS solutions in D<sub>2</sub>O

## References

- (S1) Op de Beeck, M.; Van Dyck, D.; Coene, W. Wave Function Reconstruction in HRTEM: The Parabola Method. *Ultramicroscopy* **1996**, *64*, 167–183.
- (S2) Koster, A. J.; de Jong, A. F. Measurement of the Spherical Aberration Coefficient of Transmission Electron Microscopes by Beam-Tilt-Induced Image Displacements. *Ultramicroscopy* **1991**, *38*, 235–240.
- (S3) Broek, W. Van den; Aert, S. Van; Dyck, D. Van. Fully Automated Measurement of the Modulation Transfer Function of Charge-Coupled Devices above the Nyquist Frequency. *Microsc. Microanal.* **2012**, *18*, 336–342.
- (S4) Mindell, J. A.; Grigorieff, N. Accurate Determination of Local Defocus and Specimen Tilt in Electron Microscopy. *J. Struct. Biol.* **2003**, *142*, 334–347.
- (S5) Meyer, R. R.; Kirkland, A. I.; Saxton, W. O. A New Method for the Determination of the Wave Aberration Function for High Resolution TEM 1. Measurement of the Symmetric Aberrations. *Ultramicroscopy* **2002**, *92*, 89–109.